7-2005

Membrane Potential Oscillations in Reticulospinal and Spinobulbar Neurons During Locomotor Activity

James F. Einum
Marquette University

James T. Buchanan
Marquette University, james.buchanan@marquette.edu

Journal of Neurophysiology, Vol. 94, No. 1 (July 2005): 273-281. DOI.

Membrane Potential Oscillations in Reticulospinal and Spinobulbar Neurons During Locomotor Activity

James F. Einum
Department of Biological Sciences, Marquette University, Milwaukee, Wisconsin
James T. Buchanan
Department of Biological Sciences, Marquette University, Milwaukee, Wisconsin

Abstract

Feedback from the spinal locomotor networks provides rhythmic modulation of the membrane potential of reticulospinal (RS) neurons during locomotor activity. To further understand the origins of this rhythmic activity, the timings of the oscillations in spinobulbar (SB) neurons of the spinal cord and in RS neurons of the posterior and middle rhombencephalic reticular nuclei were measured using intracellular microelectrode recordings in the isolated brain stem-spinal cord preparation of the lamprey. A diffusion barrier constructed just caudal to the obex allowed induction of locomotor activity in the spinal cord by bath application of an excitatory amino acid to the spinal bath. All of the

ipsilaterally projecting SB neurons recorded had oscillatory membrane potentials with peak depolarizations in phase with the ipsilateral ventral root bursts, whereas the contralaterally projecting SB neurons were about evenly divided between those in phase with the ipsilateral ventral root bursts and those in phase with the contralateral bursts. In the brain stem under these conditions, 75% of RS neurons had peak depolarizations in phase with the ipsilateral ventral root bursts while the remainder had peak depolarizations during the contralateral bursts. Addition of a high-Ca^{2+}, Mg^{2+} solution to the brain stem bath to reduce polysynaptic activity had little or no effect on oscillation timing in RS neurons, suggesting that direct inputs from SB neurons make a major contribution to RS neuron oscillations under these conditions. Under normal conditions when the brain is participating in the generation of locomotor activity, these spinal inputs will be integrated with other inputs to RS neurons.

INTRODUCTION

A common feature of vertebrates is the presence of descending neural systems that originate in the brain and play an important role in the control of locomotion and other movements generated by the spinal cord. These descending systems are kept informed of the state of spinal networks and of somatic sensory signals by feedback from ascending spinal pathways. In mammals, these ascending pathways influence various descending systems indirectly via the cerebellum (Orlovsky 1970b; reviewed by Arshavsky et al. 1986). In lamprey, a lower vertebrate fish, a simpler arrangement appears to exist with the majority of descending neurons originating from reticular nuclei (Swain et al. 1993; reviewed in Nieuwenhuys et al. 1998), and the ascending pathway conveying spinal locomotor network activity has direct inputs to the reticulospinal (RS) neurons (Einum and Buchanan 2004). The lamprey CNS, therefore offers a simpler organization than found in mammals for investigating the interaction of ascending pathways with the descending control system.

Rhythmic locomotor modulation of the membrane potential of RS neurons has been shown during fictive and actual locomotion in both cats (Drew et al. 1986; Orlovsky 1970a; Perreault et al. 1993) and lampreys (Deliagina et al. 2000; Dubuc and Grillner 1989; Kasicki and Grillner 1986; Kasicki et al. 1989). In the cat, ascending pathways from the spinal cord consist of the ventral spinocerebellar tract (VSCT) and the spino-reticulocerebellar pathway (SRCP), which convey activity of the spinal rhythm-generating networks (Arshavsky et al. 1978a,b; Lundberg 1971), and the dorsal spinocerebellar tract (DSCT), which conveys activity of the sensory afferents stimulated by the movements (Arshavsky et al. 1972; Lundberg and Oscarsson 1960). The cerebellum appears to extract relevant information from these ascending inputs before sending the signals on to the reticulo-, rubro-, and vestibulospinal systems (Arshavsky et al. 1986). In the lamprey, the ascending pathway consists of spinobulbar (SB) neurons (Ronan and Northcutt 1990; Vinay et al. 1998), the axons of which have been shown to be rhythmically active during fictive swimming (Vinay and Grillner 1992) and thus the SB neurons provide feedback regarding the activity of the spinal locomotor networks as is done by the VSCT and SRCP in the cat. The effect of this ascending signal in the lamprey has been demonstrated in a split-bath preparation in which fictive swimming in the spinal cord produces rhythmic oscillations of membrane potential in RS neurons (Dubuc and Grillner 1989). In contrast to the cat, this rhythmic modulation of the descending system in lamprey is not dependent on the presence of the cerebellum (Kasicki et al. 1989) and appears to involve direct inputs from the spinal cord because addition of high-Ca^{2+}, Mg^{2+} to reduce

polysynaptic pathways in the brain does not reduce the amplitude of the oscillations (Einum and Buchanan 2004).

In the control of locomotion, RS neurons are thought to be multifunctional, including involvement in the initiation and termination of locomotor activity, steering, adjustment of intensity, and postural adjustments (Deliagina and Orlovsky 2002). One hypothesis regarding the functional role of RS neurons from studies in cat suggests that they are involved in coordinating supraspinal commands with the phase of the locomotor cycle by virtue of the feedback from spinal locomotor networks (Arshavsky et al. 1986). Thus the timing of the rhythmic modulation of RS neurons in relation to the timing of activity in the locomotor networks is likely to be relevant to understanding the functional role of the feedback signals. In addition, the timing of the ascending signals responsible for the modulation of RS neurons is key to understanding how the rhythmic modulation in RS neurons is produced. In the present study, a split-bath preparation of the lamprey brain stem-spinal cord was used to characterize the timings of membrane potential oscillations in RS neurons of the posterior and middle rhombencephalic reticular nuclei (PRRN and MRRN, respectively) along with SB neurons during spinal fictive swimming and to determine whether the timings of RS neurons are dependent on polysynaptic brain stem pathways.

METHODS

Animals and dissection

The experiments were done on nine adult silver lampreys (*Ichthyomyzon unicuspis*), 28–34 cm in length, that were maintained in filtered and aerated fresh-water aquaria at ~5°C. The experiments were conducted in conformity to the American Physiological Society's *Guiding Principles in the Care and Use of Animals* and were approved by the Marquette University Institutional Animal Care and Use Committee. The animals were anesthetized by immersion in tricaine methanesulfonate (~250 mg/l, Sigma-Aldrich) prior to being transected just caudal to the last gill opening. Muscles were cut away, and a dorsal, longitudinal incision was made down the midline of the cartilage overlying the spinal cord. The dorsal portion of the cranial case was removed by making two lateral cuts that exposed the rostral spinal cord and brain stem. During dissection and experiments, the preparation was kept in normal physiological Ringer solution (8–10°C) with the following composition (in mM): 91 NaCl, 2.1 KCl, 2.6 $CaCl_2$, 1.8 $MgCl_2$, 4.0 glucose, 20 $NaHCO_3$, 8 HEPES (free acid), and 2 HEPES (sodium salt). The solution was bubbled with 98% O_2-2% CO_2, and the solution had a pH of 7.4. To provide consistent recovery following dissection, the tissue was stored overnight in Ringer at 4°C before its use in the experiment the next day.

For the experiments, the preparation was pinned to the silicone elastomer (Sylgard)-lined bottom of a cooled recording chamber perfused with normal Ringer solution (8–10°C, ~1 ml/min). A dental caulk diffusion barrier (Reprosil, Dentsply) (Dubuc and Grillner 1989) two to three segments in width was centered between the second and fifth ventral roots to separate the bath surrounding the most rostral spinal cord and brain stem from the bath surrounding the remaining cord (Fig. 1*A*). To test the integrity of the barrier, one side of the chamber was filled with Ringer solution while the other side was checked visually for leaks. If leaks were observed, the barrier was repaired with Vaseline. Once the barrier was completed, a suction electrode was placed on a ventral root caudal to the barrier (typically between VR_5 and VR_{10}), and fictive swimming was induced in the spinal cord by perfusion of either 0.3 mM *N*-

methyl-dl-aspartate (NMA) or 1 mM d-glutamate into the caudal bath. There was no significant difference observed in the phase values of reticulospinal cells using d-glutamate versus NMA ($P > 0.05$, *t*-test).

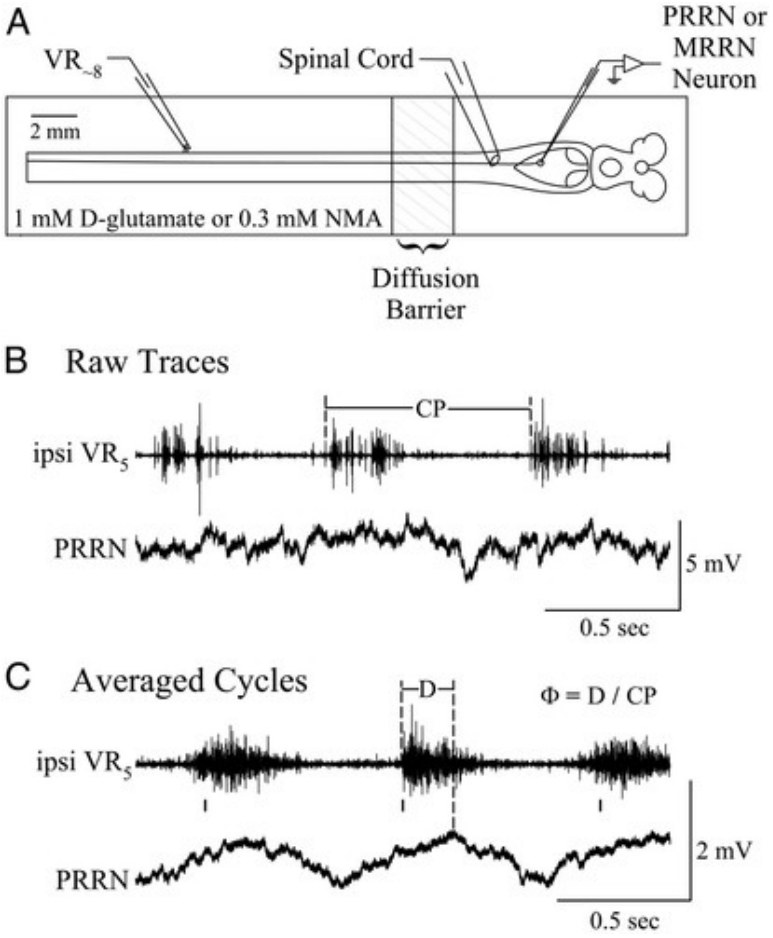

FIG. 1. Experimental approach to recording and analyzing the phases of spinal inputs to reticulospinal (RS) neurons. *A*: the in vitro preparation of the lamprey brain stem-spinal cord was divided into 2 perfusion chambers with a dental caulk barrier near the obex. Application of 1 mM d-glutamate or 0.3 mM *N*-methyl-dl-aspartate (NMA) to the spinal bath induced fictive swimming, which was monitored by a suction electrode placed on a ventral root (VR). Reticulospinal neurons of the posterior or middle rhombencephalic reticular nuclei (PRRN and MRRN, respectively) were identified by a 1:1 correspondence between an intracellular action potential and an extracellular orthodromic spike monitored by a suction electrode placed on the surface of the spinal cord near the obex. *B*: an example of an intracellular recording of a PRRN neuron and the fictive swimming activity of the ipsilateral ventral root of the 5th spinal segment. The ventral root bursting was used to measure a mean cycle period (CP) for each neuron by marking the beginnings of ventral root bursts of between 30 and 35 consecutive cycles. In this example, mean CP = 0.74 s. *C*: by triggering on the marked cycles, an average of the ventral root and the intracellular recording were made to measure the average delay of the peak of the membrane potential oscillation from the onset of the ventral root burst (*D*). This delay was divided by CP to obtain the phase relation (ϕ) for each neuron. In this cell, $\phi = 0.26$. The vertical lines below the ventral root trace indicate the time of occurrence of the ventral root bursts based on the mean CP.

Electrophysiological recordings

The membrane potentials of RS and SB neurons were recorded using sharp intracellular microelectrodes pulled on a Flaming/Brown microelectrode puller (Sutter) with resistances ranging

from 50 to 100 MΩ when filled with potassium acetate (4 M). A glass suction electrode (~300 µm inner tip diameter) was placed on the dorsal surface of the spinal cord near the obex region to identify the axonal projection of reticulospinal neurons with cell bodies in the PRRN or the MRRN. RS neurons were identified by eliciting an action potential in a neuron with intracellular current injection and detecting an orthodromic spike in the ipsilateral spinal cord recording. For some cells, averaging was necessary to detect the projection (Signal software, Cambridge Electronic Design, CED). Spinobulbar neurons were identified in a similar manner by their ascending axonal spikes recorded by a surface spinal cord electrode. In the case of SB neurons, two surface electrodes were used to determine the side of the axonal projection. All cells used for analysis had intracellular action potentials of ≥70 mV in base-to-peak amplitude. Intracellular signals were low-pass filtered at 3 kHz and amplified 50 times using an Axoclamp 2A amplifier (Axon Instruments) and a CyberAmp 320 signal conditioner (Axon Instruments). Extracellular signals were high-pass filtered at 100 Hz, low-pass filtered at 1 kHz, and amplified 10,000 times using a differential AC amplifier (A-M Systems). Digitizing was done with a micro1401 ADC converter (CED) at ≥6 kHz for intracellular and ≥2 kHz for extracellular recordings. Membrane potentials of reticulospinal cells were recorded in ~2-min blocks with a personal computer (Spike2 software, CED) and stored on disk. Some recordings were first stored on tape using a DAT recorder (Bio-Logic) and then later digitized to Spike2 files.

In a typical experiment, the membrane potentials of several PRRN and MRRN cells were sampled during fictive swimming induced in the spinal cord bath. Then the normal Ringer solution in the brain stem bath was replaced with a high-Ca^{2+} (20 mM) and high-Mg^{2+}(5.8 mM) Ringer solution to raise spike threshold to reduce polysynaptic pathways (Einum and Buchanan 2004; Frankenhaeuser and Hodgkin 1957; Rovainen 1974) and additional cells were then sampled in the PRRN and MRRN. For several RS neurons, the intracellular impalement was maintained while the normal Ringer solution surrounding the brain stem was replaced by the high-Ca^{2+}, Mg^{2+} solution.

Data analysis

Cycle period was measured from the raw ventral root bursting by manually marking the onsets of ventral root bursts of between 30 and 35 consecutive swim cycles and calculating the average time between burst onsets (Fig. 1*B*). A waveform average of each neuron's membrane potential was then obtained using the marked ventral root burst onsets as the trigger for the average. The phase relationship of membrane potential with respect to the ventral root burst cycle was defined as $\phi = D/CP$, where CP is the cycle period as measured manually from individual ventral root bursts, and *D* is the delay from the beginning of the triggered ventral root burst in the average to the peak of the membrane potential oscillation average (Fig. 1*C*). Values for ϕ will therefore range between 0 and 1. Because ϕ is determined with respect to a VR located 5–10 segments caudal to the brain stem, ϕ was adjusted to VR_1 for consistency in reporting the values. For this adjustment, a delay of 0.01 of a cycle period per segment was assumed (Wallén and Williams 1984) so that $\phi_1 = \phi_{measured} + [(n - 1) \times 0.01]$, where *n* is the VR segment number. The ϕ of SB neurons was calculated with respect to the nearest ipsilateral ventral root to the SB soma. ϕ_1 was plotted on circular plots (e.g., Fig. 3) to preserve the cyclic nature of the phase measurements. The circular plots were oriented so that the ipsi- and contralateral ventral root bursts were centered on the left and right sides of the circle, respectively. The beginning of the ipsilateral ventral root burst is defined as $\phi = 0$, and the average ventral root burst in these experiments was 0.3 of the cycle period. To distinguish ipsilateral-related phases from

contralateral-related phases, the circle was divided into halves so that peak depolarizations falling in the left (or 1st) half, 0.9–0.4, were defined as being associated with the ipsilateral ventral root burst, and peak depolarizations falling in the right (or 2nd) half, 0.4–0.9, were defined as being associated with the contralateral ventral root burst. For calculating mean phases, values between 0.9 and 0.0 were transformed to the corresponding negative values.

Statistics

For statistical comparison of RS neurons, ϕ_1 values were grouped into either the ipsilateral or contralateral halves of the cycle, and a two-way ANOVA was performed for each group. The two conditions of the ANOVA were whether the neuron was in the PRRN or MRRN and whether or not the bathing solution contained high Ca^{2+}, Mg^{2+}. Neurons within the contralateral group showed some significant differences (2-way ANOVA) so a pairwise multiple comparison procedure (Tukey test) was additionally used. For RS neurons continuously recorded before and after application of high-divalent cation solution, a paired *t*-test was performed. For all of the preceding tests, a *P* value less than or equal to 0.05 indicated a significant difference. Data are expressed as means ± SD.

RESULTS

Phase characteristics of rhythmic RS neurons in normal solution

Seventy-three RS neurons in the PRRN or the MRRN were recorded in either normal or in high-Ca^{2+}, Mg^{2+} Ringer solutions. The mean membrane potential of all RS neurons was –70 ± 9 mV, and the mean base-to-peak action potential amplitude was 93 ± 14 mV. Of these 73 neurons, 70 exhibited rhythmic membrane potential oscillations when the spinal cord was bathed in an excitatory amino acid and displayed fictive swimming. These oscillations were low in amplitude (mean = 0.7 ± 0.5 mV, *n* = 70) compared with more natural brain stem-initiated fictive swimming (mean = 5.4 mV) (Dubuc and Grillner 1989), and none of the RS neurons exhibited spiking during the spinal fictive swimming compared with the frequent spiking of RS neurons during brain stem-initiated fictive swimming (Kasicki et al. 1989).

When the brain stem was in normal Ringer solution and in a quiescent state, different RS neurons within the PRRN and MRRN showed mean peak depolarizations of membrane potential at different points in the locomotor cycle during spinal activation. Examples of the averaged membrane potentials are shown for a RS neuron in the PRRN in Fig. 2*A* and a RS neuron in the MRRN in Fig. 2*B*. For the illustrated PRRN neuron, the depolarizing peak of the oscillation occurred nearly midway in the swim cycle. In relation to the fifth ventral root, the phase of the peak depolarization of this neuron was ϕ_5 = 0.45; in relation to the first ventral root, ϕ_1 = 0.49. The illustrated MRRN neuron had a depolarizing peak at ϕ_8 = 0.20 (ϕ_1 = 0.27).

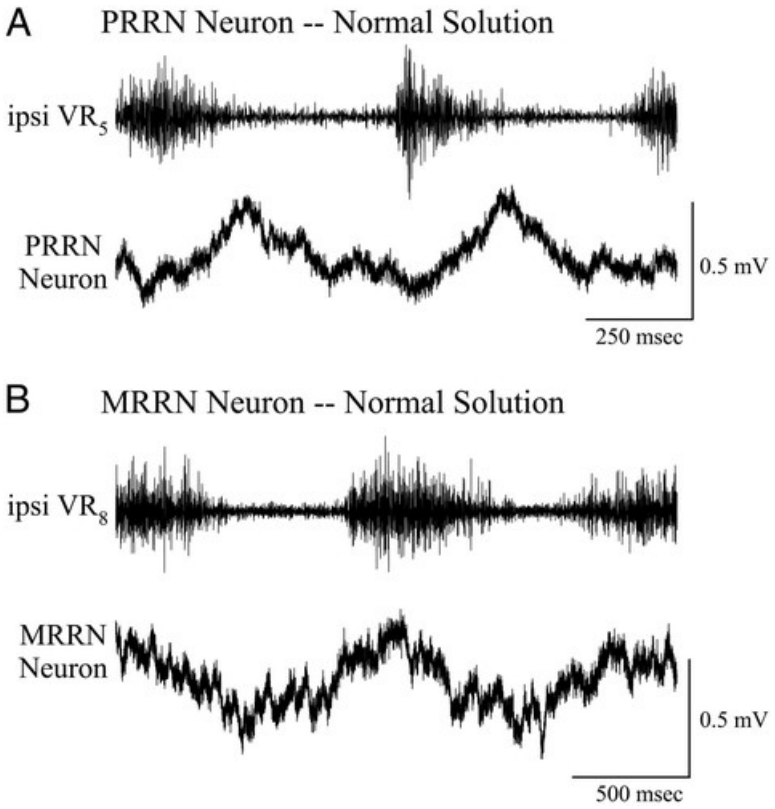

FIG. 2. Examples of the averaged membrane potential oscillations in RS neurons of the PRRN (*A*) and MRRN (*B*) in normal solution during fictive swimming of the spinal cord and an averaged ipsilateral ventral root. The ϕ of the peak depolarization in relation to the recorded ipsilateral ventral root was adjusted to the 1st ipsilateral ventral root. For the illustrated PRRN neuron in *A*, $\phi_5 = 0.45$ and $\phi_1 = 0.49$. For the illustrated MRRN neuron in *B*, $\phi_8 = 0.20$ and $\phi_1 = 0.27$.

A summary of ϕ_1 for all RS neurons recorded in the PRRN and MRRN in normal Ringer solution is shown in Fig. 3, *A* and *B*, respectively. In these circular plots, the average ipsilateral ventral root burst proportion is shown on the left (light gray), and the corresponding contralateral ventral root burst is shown on the right (dark gray). For purposes of statistical analysis, the circular plot is divided into an ipsilateral-related first half (0.9–0.4) and a contralateral-related second half (0.4–0.9). For RS neurons of the PRRN in normal solution, peak depolarizing phase values occurred in both the first and the second halves of the swim cycle. The mean of ϕ_1 in the first half was 0.24 ± 0.10 ($n = 8$), which is near the end of the ipsilateral ventral root burst. Reticulospinal neurons of the PRRN with peak depolarizations in the second half of the cycle had a mean ϕ_1 of 0.70 ± 0.15 ($n = 5$; Fig. 3*A*). Reticulospinal neurons in the MRRN had less widely distributed phases of peak depolarizations, but like the PRRN, peak depolarizations occurred in both halves of the cycle (Fig. 3*B*). Similar to the PRRN, peak depolarizations of MRRN neurons in the first half of the cycle had a mean phase value of 0.21 ± 0.04 ($n = 18$) which is in the later portion of the ipsilateral ventral root burst. Also similar to the PRRN, RS neurons of the MRRN with peak depolarizations during the contralateral-related, second half of the cycle were less common than ipsilateral-related cells. The contralateral-related RS neurons in the MRRN had a mean peak depolarization phase of 0.48 ± 0.12 ($n = 4$). There was a significant difference between RS neurons of the PRRN versus MRRN in normal Ringer for ϕ_1 during the second half of the cycle (2-way ANOVA, $P < 0.05$), but not for ϕ_1 during the first half of the cycle ($P = 0.26$).

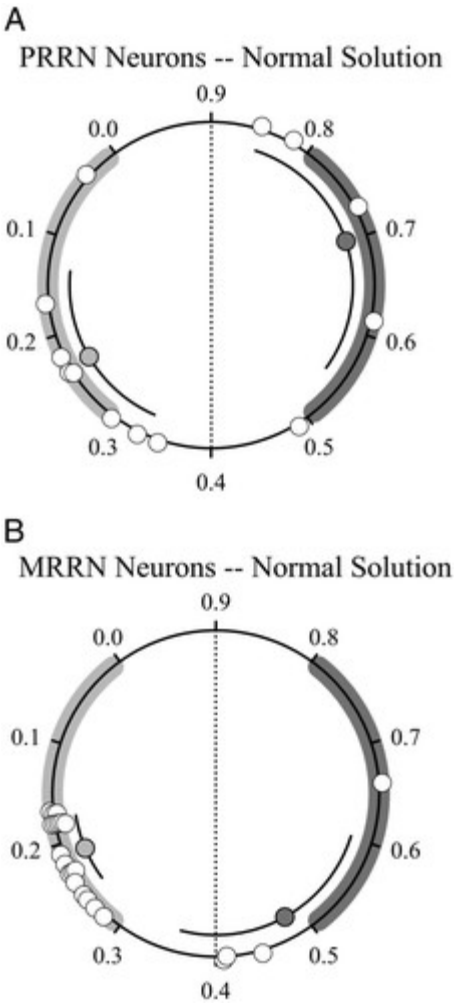

FIG. 3. Summary of the phases (ϕ_1) of the membrane potential oscillation peaks for PRRN neurons (*A*) and MRRN neurons (*B*) during fictive swimming when the brain stem was perfused with normal Ringer solution. The swim cycle is represented in a circular plot with the ipsilateral ventral root burst in light gray beginning at 0.0 and ending at 0.3. The contralateral ventral root burst is represented in dark gray from 0.5 to 0.8. The vertical dotted line divides the swim cycle into an ipsilateral-related 1st half and a contralateral-related 2nd half. ○, the ϕ_1 values for individual reticulospinal neurons; • and, mean and SD for the phase values of each half.

Phase characteristics of RS neurons in high-divalent cation solution

As previously shown using a similar experimental setup, the high-Ca^{2+}, Mg^{2+} solution reduces polysynaptic inputs with relatively less effect on monosynaptic inputs (Einum and Buchanan 2004). The high-divalent cation solution did not significantly alter the amplitude of membrane potential oscillations in RS neurons originating from the spinal cord during fictive swimming (Einum and Buchanan 2004). Therefore polysynaptic pathways involving brain stem interneurons do not appear to significantly contribute to the amplitude of the oscillations under these conditions. Such pathways, however, likely contribute to oscillations in RS neurons during brain stem-initiated activity (Kasicki and Grillner 1986; Kasicki et al. 1989). To test whether the timings of membrane potential oscillations in RS neurons are affected by reduction of polysynaptic pathways, the phases of the membrane potential oscillations were measured in high Ca^{2+}, Mg^{2+}.

As in normal Ringer solution, different RS neurons in the PRRN and MRRN in high-Ca^{2+}, Mg^{2+} solution showed peak depolarizations of membrane potential in the ipsi- or the contralateral-related halves of the cycle. An example of the averaged membrane potential for a PRRN neuron in high Ca^{2+}, Mg^{2+} is shown in Fig. 4*A* ($\phi_1 = 0.80$), and a MRRN neuron is shown in Fig. 4*B* ($\phi_1 = 0.31$). A summary of all rhythmic RS neurons in the PRRN and MRRN in high-Ca^{2+}, Mg^{2+} solution is shown in Fig. 5. Similar to their phase distributions in normal Ringer solution, the majority of PRRN neurons in high Ca^{2+}, Mg^{2+} had peak depolarizations during the first half of the cycle (mean $\phi_1 = 0.13 \pm 0.12$, $n = 17$), not significantly different from in normal solution ($P = 0.07$). Neurons that had peak depolarizations in the second half were less common ($n = 4$) and had a mean ϕ_1 of 0.78 ± 0.09, again not significantly different from normal solution ($P = 0.46$). Reticulospinal neurons of the MRRN with high-Ca^{2+}, Mg^{2+}

solution surrounding the brain stem also displayed peak depolarizations of membrane potential in either half of the locomotor cycle. Although the mean ϕ_1 of neurons in the first half of the cycle, 0.22 ± 0.13 (*n* = 9), was not significantly different from control (*P* = 0.07), MRRN neurons in high Ca^{2+}, Mg^{2+} had values later in the second half. The mean ϕ_1 of this group, 0.71 ± 0.19 (*n* = 5), was significantly different from the contralateral-related group in normal solution (0.48 ± 0.12; *n* = 4) for MRRN neurons (2-way ANOVA, *P* = 0.03) suggesting that polysynaptic pathways in the brain stem may play a role in determining membrane potential oscillation timing of some MRRN neurons.

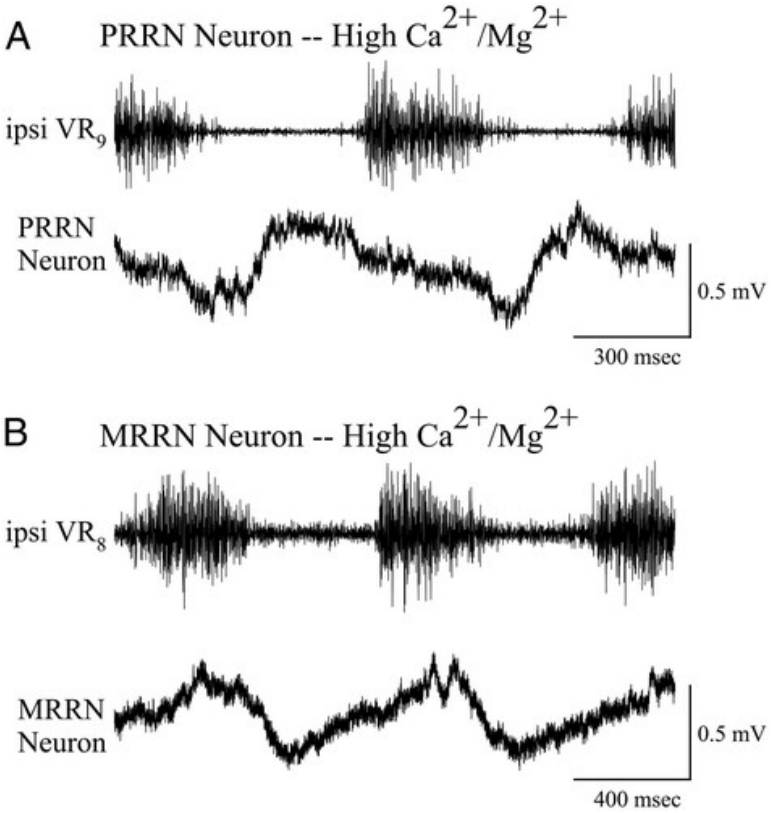

FIG. 4. Examples of the averaged membrane potential oscillations in reticulospinal neurons of the PRRN (*A*) and MRRN (*B*) in high-Ca^{2+}, Mg^{2+} solution during fictive swimming of the spinal cord. For the illustrated PRRN neuron in *A*, ϕ_9 = 0.72 and ϕ_1 = 0.80. For the illustrated MRRN neuron in *B*, ϕ_8 = 0.24 and ϕ_1 = 0.31.

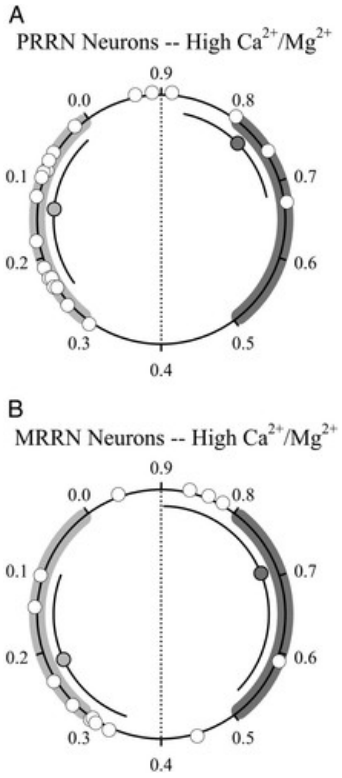

FIG. 5. Summary of the phases (ϕ_1) of the membrane potential oscillation peaks for PRRN neurons (*A*) and MRRN neurons (*B*) during fictive swimming while the brain stem was perfused with high-Ca^{2+}, Mg^{2+} Ringer solution.

In sum, no differences were found between the mean phase values of RS neurons with peak depolarizations during the first half of the cycle, either in normal or in high-divalent cation solution. In normal solution, a difference was found between contralateral-related PRRN and contralateral-related MRRN neurons, with the latter occurring earlier in the second half of the cycle. In addition, contralateral-related MRRN neurons differed in high Ca^{2+}, Mg^{2+} versus in normal solution.

Phase characteristics of individual RS neurons

Three RS neurons in the PRRN and one RS neuron in the MRRN were impaled in normal Ringer solution, and the impalements were continuously maintained during replacement of this solution with the high-Ca^{2+}, Mg^{2+} solution. Phase values were obtained for each neuron before and during high Ca^{2+}, Mg^{2+}, and a paired *t*-test was performed on these cells ($n = 4$). No significant difference was found before and after the high divalent treatment for the phase values ($P = 0.5$). These neurons included ipsilateral-related PRRN and MRRN neurons and two contralateral-related PRRN neurons.

Phase characteristics of spinobulbar neurons

The source of rhythmic spinal input to reticulospinal neurons in the split-bath preparation is the SB neurons. Therefore the membrane potential activity of SB neurons ($n = 21$) during fictive locomotion was measured with intracellular microelectrodes, and their activities were related to the bursting in the nearest ipsilateral ventral root. The SB neurons could be either ipsilaterally projecting (iSB) or contralaterally projecting (cSB).

The mean membrane potential for SB neurons was –70 ± 8 mV, and the mean base-to-peak amplitude of their action potentials was 86 ± 14 mV. On average, the SB neurons had significantly greater membrane potential oscillation amplitudes than the RS neurons ($P < 0.001$; Fig. 6). The mean peak-to-trough amplitude for all SB neuron oscillations was 3.8 ± 3.2 mV ($n = 21$) and ranged from 0.7 to 14 mV. The mean oscillation amplitude of iSB neurons (4.2 ± 3.2 mV; $n = 8$) was not significantly different from the mean amplitude of cSB neurons (3.5 ± 3.4 mV; $n = 13$; $P = 0.6$). Only 4 of the 21 SB neurons exhibited spiking during fictive swimming. The spiking SB neurons fired one to three spikes per swim cycle on the crests of their depolarizations. These cells included two iSB and two cSB neurons. An example of a spiking iSB neuron is shown in Fig. 6*A*. The percentage of SB neurons exhibiting spiking (19%) is likely an underestimate due to an inherent sampling bias toward larger neurons. In addition, the more vigorous fictive swimming activity initiated by the brain stem would likely recruit more SB neurons to spiking.

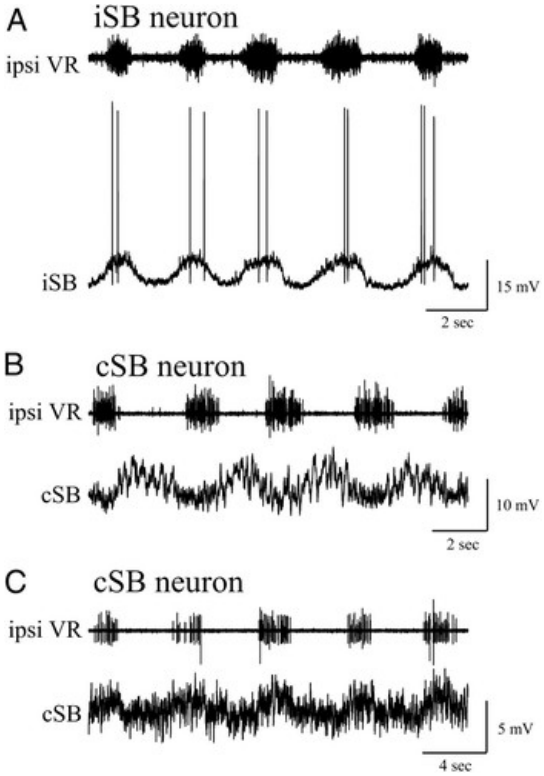

FIG. 6. Examples of rhythmic membrane potential activity of SB neurons during fictive swimming. *A*: ipsilaterally projecting SB (iSB) neuron that was 1 of 4 SB neurons exhibiting spiking during fictive swimming. This cell was in phase with the nearby ipsilateral ventral root as were all recorded iSBs. *B*: a contralaterally projecting SB (cSB) neuron that was out of phase with the nearby ipsilateral ventral root. *C*: a contralaterally projecting SB neuron that was in phase with the nearby ipsilateral ventral root. The cSBs were about equally divided between the in phase and out of phase cells.

Phases of membrane potential peaks for iSB neurons were plotted separately from phase values obtained from cSB neurons (Fig. 7). The phases of peak depolarizations of iSB neurons ($n = 8$) ranged from 0.01 to 0.25 with a mean of 0.13 ± 0.08. Thus all tested iSB neurons were in phase with the nearby ventral root burst (Figs. 6*A* and 7*A*). In contrast, cSB neurons had a broader distribution of phase values of peak depolarizations including both ipsilateral-related and contralateral-related cSB cells. The mean phase of the membrane potential oscillation peaks for ipsilateral-related cSB neurons

was 0.21 ± 0.10 (*n* = 6; Figs. 6*C* and 7*A*); the mean phase value for contralateral-related cSB neurons was 0.69 ± 0.16 (*n* = 7; Figs. 6*B* and 7*B*). There was no significant difference between the mean peak depolarization phase of iSB and the ipsilateral-related cSB neurons (*P* = 0.09).

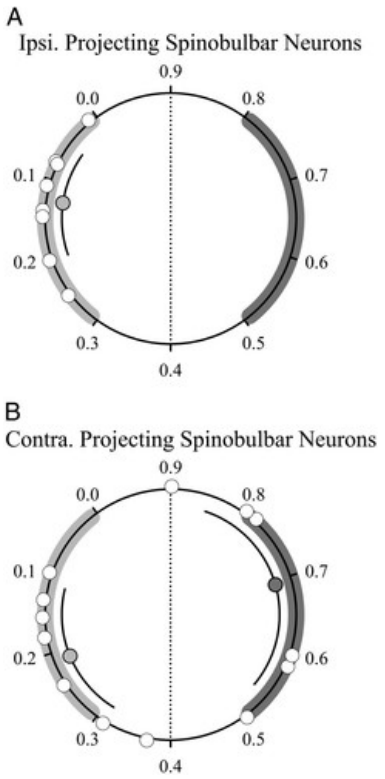

FIG. 7. Summary of the phases (ϕ) of the membrane potential oscillation peaks for ipsilaterally projecting (*A*) and contralaterally projecting (*B*) SB neurons during fictive swimming. The ϕ for each neuron was measured with respect to the nearby ipsilateral ventral root.

Conduction velocity of spinobulbar neurons

The conduction velocity of SB neurons will determine the time it takes for a spinobulbar signal to reach the brain stem and could affect the timing patterns observed in RS neurons. The range of observed conduction velocities was 0.10–1.52 m/s for SB neurons, and the mean was 0.8 ± 0.4 m/s (*n* = 21). There was no significant difference between the mean conduction velocities of iSB and cSB neurons (0.80 ± 0.36 vs. 0.77 ± 0.45 m/s, respectively; *P* = 0.86). In the brain stem/spinal cord preparation used here, the caudal-most SB neurons recorded were 30 mm from the brain stem, so that, on average, signals from the most caudal of these cells would take 40 ms (range = 20–300 ms) to reach the brain stem. Considering that the mean cycle period for the experiments involving recordings of SB neurons was 2.3 ± 1.8 s, a 40-ms delay is <2% of the cycle period. Thus the conduction velocity of SB neurons of the gill region is not likely to be an important determinant of the timing of the oscillatory input to RS neurons. However, at faster swim rates, some SB neurons may have sufficiently long conduction times to significantly affect the phase of their input to the RS neurons.

DISCUSSION

This study has shown that ascending spinal activity during fictive locomotion produces rhythmic membrane potential oscillations in RS neurons that exhibit a wide range of phase relations to the

rhythmic activity of the first spinal ventral root. In both the MRRN and the PRRN, the membrane potential oscillations of most individual RS neurons were in phase with the ipsilateral ventral root, but ~25% of RS neurons had membrane potential oscillations in phase with the contralateral ventral root. After reducing polysynaptic pathways in the brain stem by applying a high-divalent cation solution, there was a similar distribution of RS neuron membrane potential oscillation phase relationships, suggesting that the timings of the RS membrane potential modulations are determined largely by monosynaptic spinobulbar inputs under these conditions. The exception was MRRN neurons that had peak depolarizations in phase with the contralateral ventral root in normal solution. The phase of the peak depolarizations of these cells was different in high-divalent cation indicating the possible involvement of polysynaptic brain stem pathways.

The SB neurons were also rhythmically active during fictive locomotion and had significantly larger amplitude oscillations than RS neurons. Like the RS neurons, the SB neurons exhibited a range of membrane potential oscillation phase relations to the nearby ventral root bursts: ipsilaterally projecting SB neurons were all in phase with the ipsilateral burst, whereas contralaterally projecting SB neurons were about evenly divided between those related to the ipsilateral burst and those related to the contralateral burst.

Comparison with previous studies

A recent study evaluated the amplitudes of membrane potential oscillations of RS neurons in a split bath experiment before and after addition of a high-divalent cation solution (Einum and Buchanan 2004). This previous study demonstrated that polysynaptic pathways are significantly reduced with the high-Ca^{2+}, Mg^{2+} solution with only a slight reduction in monosynaptic connections. However, the amplitudes of the membrane potential oscillations in RS neurons were not significantly altered by this high-divalent solution suggesting mainly direct input from the spinal cord to the RS neurons. Similarly in the present study, the timings of the oscillations were, for the most part, not affected by the high-divalent cation solution. The exception was the contralateral-related RS neurons of the MRRN, which exhibited a significantly different mean phase in normal solution compared with high-divalent cation, possibly indicating involvement of polysynaptic brain stem pathways. Overall, while the present study cannot rule out the participation of interneuronal pathways within the brain stem, the results are consistent with the proposal that direct connections from SB neurons to RS neurons exist. However, one must bear in mind that when the brain stem initiates locomotor activity, the level of excitation among RS neurons is considerably greater (5.4 mV, peak to trough amplitude) (Dubuc and Grillner 1989) than that found in the split bath preparation [2.2 mV in Dubuc and Grillner (1989); 0.7 mV in the present study]. If interneuronal pathways exist, one might expect their greater participation during the more intense activity of brain stem-initiated locomotor activity compared with the split bath preparation in which the brain stem is quiescent. It is also possible that the distribution of phase relationships in RS neurons may well change under brain stem-initiated locomotor activity.

Previous work suggested that the modulations of RS neuron membrane potentials in the MRRN and PRRN of lamprey were all in phase with the ipsilateral ventral root bursts during fictive swimming (Dubuc and Grillner 1989; Kasicki and Grillner 1986; Kasicki et al. 1989) in contrast to the present finding that ~25% of RS neurons had peak depolarizations during the contralateral burst. This difference is most likely due to the use of averaging in the present study, allowing detection of

rhythmic activity in cells that might otherwise be regarded as nonrhythmic. It is also possible that during brain-stem-initiated fictive swimming activity, the phase relationships of RS neurons may be different as the ascending signals become integrated with brain signals and with additional SB neurons recruited during the more vigorous fictive swimming activity. During actual locomotion of lampreys, recordings of RS axons in the spinal cord found that the spiking of RS neurons is often rhythmically active, usually in phase with the ipsilateral ventral root (Deliagina et al. 2000). Occasionally, however, individual axons on opposite sides of the spinal cord were observed to be active in phase with one another. If these RS neurons both had ipsilateral axons, this would suggest that some RS cell bodies are spiking in phase with the contralateral ventral roots (Deliagina et al. 2000). In vestibulospinal neurons, ~20% of the cells had rhythmic activity in phase with the contralateral ventral root, and these cells were found to project to the opposite side of the spinal cord (Bussières and Dubuc 1992). Consistent with this latter observation, the contralaterally projecting Mauthner cells of the brain stem have rhythmic activity in phase with the contralateral ventral roots (Kasicki et al. 1989).

A previous study of the timings of SB neuron rhythmic activity was done by Vinay and Grillner (1992) in which axons of SB neurons were recorded intracellularly during fictive locomotion. An analysis of the timings of the spikes revealed a range of phase relationships including those active in phase with either the ipsi- or contralateral ventral roots and about a third of the axons were active at the transitions between ipsi- and contralateral bursts. Although these results are not inconsistent with the present study, the two studies are not directly comparable because the locations of the cell bodies of origin of the recorded axons were not determined in the Vinay and Grillner study. A more comparable study was done with an intracellular recording from the cell body of a single contralaterally projecting SB neuron (Vinay et al. 1998). This cell exhibited rhythmic membrane potentials and spiking that were in phase with the contralateral ventral root. This is consistent with the findings of the present study that about half of the contralaterally projecting SB neurons had rhythmic activity in phase with the contralateral ventral root. Also consistent with these two previous reports, the present study found that some SB neurons fire action potentials during fictive locomotion. Only ~20% of the recorded SB neurons did so, however, presumably indicating a large reserve of SB neurons for recruitment during more intense swimming activity.

Functional implications

Rhythmic modulation of the membrane potential of RS neurons may serve to coordinate or gate the timing of RS neuron firing with particular phases of the locomotor cycle. For example, during actual locomotion, vestibular inputs to RS neurons produced by tilts of the lamprey are superimposed on the rhythmic activity in the RS neurons so that the resulting output of the RS neuron during tonic vestibular input is phasic rather than the tonic output observed when the animal is not swimming (Deliagina et al. 2000). Thus the various sensory modalities that converge onto RS neurons will be to some extent transformed into a rhythmic output by the RS neuron during locomotion. The observation here that ~25% of the RS neurons are related to the contralateral ventral root burst suggests that this transforming process varies considerably among RS neurons. There are several important pieces of information, however, that will be needed to further understand the functional consequences of this multi-phasic modulation. One is a clear determination of whether these RS neurons with activity phases related to the contralateral bursting have a similar phase during brain-stem-initiated locomotor activity. It will also be important to determine whether contralaterally-related RS neurons have a

contralateral descending axon. Based on retrograde labeling studies, ≤20% of RS neurons have contralateral descending axons (Ronan 1989). Our method of identifying RS neurons with a surface electrode on the ipsilateral side of the cord could not exclude the possibility that the axon actually projected contralaterally with signal spread to the ipsilateral electrode. It will also be necessary to relate the phase of rhythmic activity of the RS neuron to the sign of its synaptic output. Although most RS neurons are excitatory (Ohta and Grillner 1989), inhibitory glycinergic RS neurons have also been demonstrated (Wannier et al. 1995). Ultimately, to understand the functional significance of the rhythmic modulation, it will be necessary to have some further insight into the roles of individual RS neurons in the spinal cord.

An advance in understanding the functional roles of individual RS neurons during locomotion in lamprey has emerged recently (Zelenin et al. 2001, 2003). In these studies, individual RS neurons in various nuclei were stimulated repetitively while recording the dorsal and ventral branches of the ventral root innervating, respectively, dorsal and more ventrally located body muscles. Spike-triggered averaging from tonically stimulated RS neurons revealed that individual RS neurons produce particular patterns of excitation and inhibition among the dorsal and ventral branches of the two sides of the cord. ≥20 different patterns of excitation and inhibition were observed, and these could be divided into seven different functional groups according to the direction of body bending that would result. These patterns may represent different muscle synergies underlying motor behaviors such as turning. In relation to the present study, the actual pattern produced by a single RS neuron during locomotion will depend critically on the phase of its rhythmic activity.

A previous study (Kasicki et al. 1989) proposed that precise rhythmic timing information of RS neuron population activity will be lost as it descends the length of the spinal cord except in the most rostral segments of the spinal cord. This loss is expected on the basis of the wide range of RS axonal conduction velocities (0.1–5 mm/ms), the long conduction distances (~200 mm in a typical animal), and the slow propagation of locomotor network activity down the spinal cord (intersegmental phase lag of 1% of the cycle period per segment) (Wallén and Williams 1984). As a consequence of these factors, the rhythmic firing of RS neurons would be spread throughout the swim cycle at segments more caudal than the first 10–20 (of 100 total spinal segments). In the most rostral spinal cord, axonal conduction delays and intersegmental phase lag would be relatively small fractions of the cycle period, and thus timing information would be preserved. As previously pointed out (Kasicki et al. 1989), the rostral region of the spinal cord is likely to be of key importance in the control of steering, equilibrium, and speed of swimming because changes produced by RS inputs to the rostral locomotor networks would then propagate to the remainder of the spinal cord via intersegmental coupling.

The wide range of phases observed here for the oscillatory activity in SB neurons indicates that the range of phases in the RS neurons during pharmacological spinal activation can be accounted for by input from the SB neurons. Clearly, it will be necessary to link phase information of SB neurons with their synaptic sign and their target RS neurons to provide a full account of the SB-dependent RS neuron modulation. At least one prediction can be made from the observations here: some contralaterally projecting SB neurons are likely to have excitatory outputs. Given the existence of RS neurons that are rhythmically active in phase with the contralateral ventral roots, the observation that rhythmic modulation of RS neurons is due to both excitatory and inhibitory inputs (Dubuc and Grillner 1989;

Einum and Buchanan 2004) and that all observed ipsilaterally-projecting SB neurons are active in phase with the ipsilateral ventral root, it follows that the excitatory phase occurring with the contralateral ventral roots would originate from contralaterally projecting SB neurons. There is a precedent for excitatory cSB neurons in lamprey: the giant interneurons are a class of contralaterally projecting SB neurons in the caudal region of spinal cord that have excitatory synaptic outputs to at least one class of RS neurons (Rovainen 1967, 1974). Some giant interneurons exhibit rhythmic membrane potentials during fictive swimming (Buchanan and Cohen 1982). Clearly, it will be important to determine the sign of synaptic output for the different SB neurons observed here and their interactions with RS neurons in determining whether they may be subdivided into functional groupings in terms of patterns of effects on ventral root branches during locomotor activity. Finally, it will be important to understand how these ascending signals are integrated with other inputs to the RS neurons during locomotor activity.

Conclusions

Similar to mammals, the lamprey ascending system conveys rhythmic signals to the brain stem concerning the activity of the spinal locomotor network. However, rather than indirectly modulating the membrane potential of descending neurons via the cerebellum, the present study supports the proposal that some spinobulbar neurons make direct connections on RS neurons in lamprey. The rhythmic activity of RS neurons that is generated by SB neurons may serve to gate descending commands to particular phases of the locomotor cycle in the rostral spinal cord. The wide range of the timings of this rhythmic activity in different RS neurons suggests that they may be subdivided according to different functional effects and that the ascending spinobulbar neurons generating these rhythmic modulations may also be similarly organized.

GRANTS

This work was supported by National Institute of Neurological Disorders and Stroke Grant NS-40755 to J. T. Buchanan.

FOOTNOTES

- The costs of publication of this article were defrayed in part by the payment of page charges. The article must therefore be hereby marked "*advertisement*" in accordance with 18 U.S.C. Section 1734 solely to indicate this fact.

AUTHOR NOTES

- Address for reprint requests and other correspondence: J. T. Buchanan, Dept. of Biological Sciences, Marquette University, P.O. Box 1881, Milwaukee, WI 53201 (E-mail: james.buchanan@marquette.edu)

REFERENCES

Arshavsky et al. 1972 Arshavsky YI**, Berkinblit MB, Fukson OI, Gelfand IM, and Orlovsky GN.** Recordings of neurons of the dorsal spinocerebellar tract during evoked locomotion. ***Brain Res*** *43*: 272–275, 1972.

Arshavsky et al. 1986 Arshavsky YI**, Gelfand IM, and Orlovsky GN.** ***Cerebellum and Rhythmical Movements.*** New York: Springer, 1986.

Arshavsky et al. 1978a Arshavsky YI**, Gelfand IM, Orlovsky GN, and Pavlova GA.** Messages conveyed by spinocerebellar pathways during scratching in the cat. I. Activity of neurons of the lateral reticular nucleus. ***Brain Res*** *151*: 479–491, 1978a.

Arshavsky et al. 1978b Arshavsky YI**, Gelfand IM, Orlovsky GN, and Pavlova GA.** Messages conveyed by spinocerebellar pathways during scratching in the cat. II. Activity of neurons of the ventral spinocerebellar tract. ***Brain Res*** *151*: 493–506, 1978b.

Arshavsky et al. 1988 Arshavsky YI**, Orlovsky GN, and Perret C.** Activity of rubrospinal neurons during locomotion and scratching in the cat. ***Behav Brain Res*** *28*: 193–199, 1988.

Buchanan and Cohen 1982 Buchanan JT **and Cohen AH.** Activities of identified interneurons, motoneurons, and muscle fibers during fictive swimming in the lamprey and effects of reticulospinal and dorsal cell stimulation. ***J Neurophysiol*** *47*: 948–960, 1982.

Bussières et al. 1992 Bussières N**, and Dubuc R.** Phasic modulation of vestibulospinal neuron activity during fictive locomotion in lampreys. ***Brain Res*** *575*: 174–179, 1992.

Deliagina and Orlovsky 2002 Deliagina TG **and Orlovsky GN.** Comparative neurobiology of postural control. ***Curr Opin Neurobiol*** *12*: 652–657, 2002.

Deliagina et al. 2000 Deliagina TG**, Zelenin PV, Fagerstedt P, Grillner S, and Orlovsky GN.** Activity of reticulospinal neurons during locomotion in the freely behaving lamprey. ***J Neurophysiol*** *83*: 853–863, 2000.

Drew et al. 1986 Drew T**, Dubuc R, and Rossignol S.** Discharge patterns of reticulospinal and other reticular neurons in chronic, unrestrained cats walking on a treadmill. ***J Neurophysiol*** *55*: 375–401, 1986.

Dubuc and Grillner 1989 Dubuc R **and Grillner S.** The role of spinal cord inputs in modulating the activity of reticulospinal neurons during fictive locomotion in the lamprey. ***Brain Res*** *483*: 196–200, 1989.

Einum and Buchanan 2004 Einum JF **and Buchanan JT.** Reticulospinal neurons receive direct spinobulbar inputs during locomotor activity in lamprey. ***J Neurophysiol*** *92*: 1384–1390, 2004.

Frankenhaeuser and Hodgkin 1957 Frankenhaeuser B **and Hodgkin AL.** The action of calcium on the electrical properties of squid axons. ***J Physiol*** *137*: 218–244, 1957.

Kasicki and Grillner 1986 Kasicki S **and Grillner S.** Müller cells and other reticulospinal neurones are phasically active during fictive locomotion in the isolated nervous system of the lamprey. ***Neurosci Lett*** *69*: 239–243, 1986.

Kasicki et al. 1989 Kasicki S**, Grillner S, Ohta Y, Dubuc R, and Brodin L.** Phasic modulation of reticulospinal neurons during fictive locomotion and other types of spinal motor activity in lamprey. ***Brain Res*** *484*: 203–216, 1989.

Lundberg 1971 Lundberg A**.** Function of the ventral spinocerebellar tract. A new hypothesis. ***Brain Res*** *12*: 317–330, 1971.

Lundberg and Oscarsson 1960 Lundberg A **and Oscarsson O.** Functional organization of the dorsal spino-cerebellar tract in the cat. VII. Identification of units by antidromic activation from the cerebellar cortex with recognition of five functional subdivisions. ***Acta Physiol Scand*** *50*: 356–374, 1960.

Nieuwenhuys et al. 1998 Nieuwenhuys R**, ten Donkelaar HJ, and Nicholson C.** ***The Central Nervous System of Vertebrates.*** New York: Springer, 1998, vol 1.

Ohta and Grillner 1989 Ohta Y **and Grillner S.** Monosynaptic excitatory amino acid transmission from the posterior rhombencephalic reticular nucleus to spinal neurons involved in the control of locomotion in lamprey. ***J Neurophysiol*** *62*: 1079–1089, 1989.

Orlovsky 1970a Orlovsky GN**.** Work of the reticulo-spinal neurones during locomotion. ***Biophysics USSR*** *15*: 761–771, 1970a.

Orlovsky 1970b Orlovsky GN**.** Influence of the cerebellum on the reticulo-spinal neurons during locomotion. ***Biophysics USSR*** *15*: 928–936, 1970b.

Orlovsky 1972a Orlovsky GN**.** Activity of vestibulospinal neurons during locomotion. ***Brain Res*** *46*: 85–98, 1972a.

Orlovsky 1972b Orlovsky GN**.** Activity of rubrospinal neurons during locomotion. ***Brain Res*** *46*: 99–112, 1972b.

Perreault et al. 1993 Perreault MC**, Drew T, and Rossignol S.** Activity of medullary reticulospinal neurons during fictive locomotion. ***J Neurophysiol*** *69*: 2232–2247, 1993.

Ronan 1989 Ronan M**.** Origins of the descending spinal projections in petromyzontid and myxinoid agnathans. ***J Comp Neurol*** *281*: 54–68, 1989.

Ronan and Northcutt 1990 Ronan M **and Northcutt G.** Projections ascending from the spinal cord to the brain in petromyzontid and myxinoid agnathans. ***J Comp Neurol*** *291*: 491–508, 1990.

Rovainen 1967 Rovainen CM**.** Physiological and anatomical studies on large neurons of central nervous system of the sea lamprey (*Petromyzon marinus*). II. Dorsal cells and giant interneurons. ***J Neurophysiol*** *30*: 1024–1042, 1967.

Rovainen 1974 Rovainen CM**.** Synaptic interactions of reticulospinal neurons and nerve cells in the spinal cord of the sea lamprey. ***J Comp Neurol*** *154*: 207–224, 1974.

Swain et al. 1993 Swain GP**, Snedeker JA, Ayers J, and Selzer ME.** Cytoarchitecture of spinal-projecting neurons in the brain of the larval sea lamprey. ***J Comp Neurol*** *336*: 194–210, 1993.

Vinay et al. 1998 Vinay L**, Bussières N, Shupliakov O, Dubuc R, and Grillner S.** Anatomical study of spinobulbar neurons in lampreys. ***J Comp Neurol*** *397*: 475–492, 1998.

Vinay and Grillner 1992 Vinay L **and Grillner S.** Spino-bulbar neurons convey information to the brainstem about different phases of the locomotor cycle in the lamprey. ***Brain Res*** *582*: 134–138, 1992.

Wallén and Williams 1984 Wallén P **and Williams TL.** Fictive locomotion in the lamprey spinal cord in vitro compared with swimming in the intact and spinal animal. ***J Physiol*** *347*: 225–239, 1984.

Wannier et al. 1995 Wannier T**, Orlovsky G, and Grillner S.** Reticulospinal neurones provide monosynaptic glycinergic inhibition of spinal neurons in lamprey. ***Neuroreport*** *6*: 1597–1600, 1995.

Zelenin et al. 2001 Zelenin PV**, Grillner S, Orlovsky GN, and Deliagina TG.** Heterogeneity of the population of command neurons in the lamprey. ***J Neurosci*** *21*: 7793–7803, 2001.

Zelenin et al. 2003 Zelenin PV**, Pavlova EL, Grillner S, Orlovsky GN, and Deliagina TG.** Comparison of the motor effects of individual vestibulo- and reticulospinal neurons on dorsal and ventral myotomes in lamprey. ***J Neurophysiol*** *90*: 3161–3167, 2003.